Influence of global geophysical processes on variability of ozone, temperature, and aerosol vertical distribution over West Siberia

G.M. Kruchenitskii[1] and V.N. Marichev[2]

[1]*Central Aerological Observatory, RosHydroMet, Dolgoprudnyi*
[2]*Institute of Atmospheric Optics, Siberian Branch of the Russian Academy of Sciences, Tomsk*

Received August 23, 2007

Based on lidar sounding of ozone, aerosol, and temperature in the stratosphere over Tomsk, the influence of the world centers of action on their vertical distribution has been investigated through constructing regression models, which include parameters, such as month-average profiles of ozone, aerosol, and temperature. As regressors, the state of the world action centers and surface temperature of some areas of the World Ocean were used. Regressor values were used with zero and month lags. This approach significantly increased the modeling efficiency (the values of determination coefficients in regression models) as compared to the initial results. Moreover, the use of regressor values with a nonzero lag enabled the evaluation of the time constant for processes governing the influence of the world action centers on the temperature, ozone concentration, and optical activity of aerosol at different heights.

Introduction

In our earlier work[1] the results of estimation of influence of the global geophysical factor (GGF) on the ozone vertical distribution (OVD) and the temperature vertical distribution (TVD) over West Siberia were considered. Those estimations were based on the data of lidar sounding in Tomsk during winter period from 1996 to 2000, and were used in building the regressive model for monthly mean profiles of OVD and TVD. In this article the regressive model is modified at the expense of the inclusion of GGF values with a month lag in the list of regressors. The profiles of aerosol vertical distribution (AVR) were additionally included as model ones.

1. Initial data

The sensing altitude range was 10–50 km. The distribution of the initial data is presented in Fig. 1.

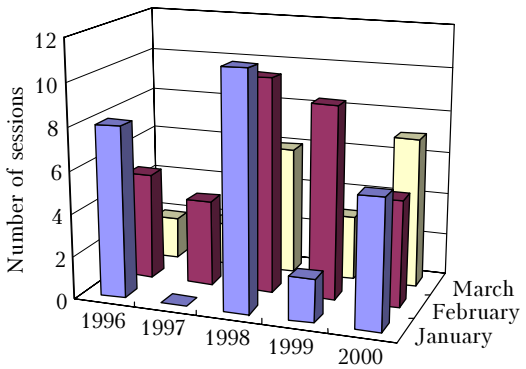

Fig. 1. Monthly number of lidar sensing sessions.

Figure 2 exemplifies profiles of the ratio of total aerosol and molecular backscattering to inverse molecular backscattering, as well as the ozone vertical distribution and the temperature.

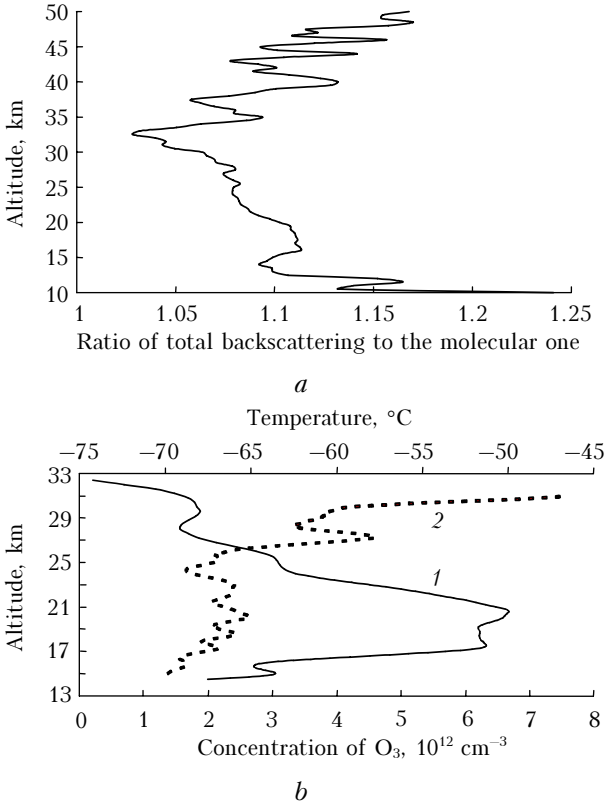

Fig. 2. An example of lidar sensing results (January 26, 1996): AVR (*a*), OVD (*b*, *1*), and TVD (*b*, *2*).

0235-6880/08/04 257-05 $02.00

As the regressors, we tested solar activity index $F_{10.7}$ (ftp://ftp.ngdc.noaa.gov/STP/SOLAR_DATA/SOLAR_RADIO/FLUX/), as well as different atmospheric and oceanic indices (http://www.cpc.ncep.noaa.gov/), computed by the National Climate Prediction Center – NCEP USA. All regressors, as well as the modeled values of complete scattering ratio to the molecular one are presented as the series averaged over 1 month interval. Among them are:

– indices of equator-mean zonal wind at levels of 30 (w30) and 50 (w50) mbar (analogous of the zonal wind in Singapore) – QBO_{30} and QBO_{50} respectively;

– indices of Southern (SOI), Arctic (AO), North Atlantic Pacific (NAO), North Atlantic and Antarctic Atlantic (PNA and AAO) vibrations;

– ocean surface temperatures: Pacific – Nino 1+2 (0–10S, 90W–80W), Nino 3 (5N–5S, 150W–90W), Nino 3.4 (5N–5S, 170–120W), Nino 4 (5N–5S, 160E–150W) and Atlantic: North Atlantic (5–20N, 60–30W), South Atlantic (0–20S, 30W–10E), and Tropical Atlantic (10N–10S, 180W–180E). The names are very conditional, because reflect the position of the corresponding Atlantic area relative to equator and do not coincide with the traditional geographical terms);

– mean zonal temperature (z500t) at the level of 500 gPa;

– outgoing long-wave radiation (OLR) at the equator (160E–160W). A more detailed description of the regressors can be found at the above-mentioned site. In addition to the listed regressors we also used the QBO_{30} – $r_s(t)$ envelope obtained from zonal wind index $s(t)$ by its transmission through a numerically synthesized heterodyne detector. This envelope is connected with the indicated index by the relation

$$r_s(t) \sim a \int_0^\infty s(\tau)\sin(2\pi f_g \tau) \times$$

$$\times \left[\frac{\sin 2\pi F(t-\tau)}{t-\tau} + \frac{\sin 2\pi F(t+\tau)}{t+\tau} \right] d\tau, \qquad (1)$$

where $f_g = 1/28$ month^{-1} is the heterodyne frequency; $F = 1/132$ month^{-1} is the upper boundary of a low frequency filter's transmission band.

Let us give some explanations. Usually, QBO_{50} is used along with QBO_{30} as regressors in statistical modeling of ozonosphere processes. In this case both vibrations are shifted relative to each other by 7 months, i.e., a quarter of QBO main (carrier) frequency period, equal to 28 months (hereafter $f_g = 1/28$ month[1]). Thus, the QBO_{30} and QBO_{50} couple is an analog of sine and cosine in a common harmonic expansion. When isolating the QBO envelope, phase peculiarities of the signal at the carrier frequency are taken into account by the sine and cosine heterodyne phasing. When the QBO_{50} is demodulated through the heterodyne sine phasing, than the receiver's yield is practically the same as in the case of QBO_{30} heterodyning with the use of cosine phasing, and vice versa. The envelope obtained at heterodyne cosine phasing for QBO_{30} envelope selection, turned out to be insignificant regressor for all analyzed processes.

2. Building of model

AVR, OVD, and TVD deviations from the month-average values, obtained by inter-annual averaging (remnants of seasonal behavior), were modeled. All regressors were used in a normalized form, i.e., after their centering to zero mean and normalizing to a unit variance. Because of a limited time period of the initial series and a significant amount of tested regressors, the modeling was carried out with the help of a special recursion procedure, which ranged the regressors according to their statistical importance. Further, the contribution of the most significant regressor was excluded by this procedure from the modeled process; as well as the regressor itself was excluded from the list of the remnants tested in the process of modeling. The procedure was terminated when the value of the Student's statistics for the most significant regressor exceeded 5%. The process chart of the regressive model building algorithm is presented in Fig. 3.

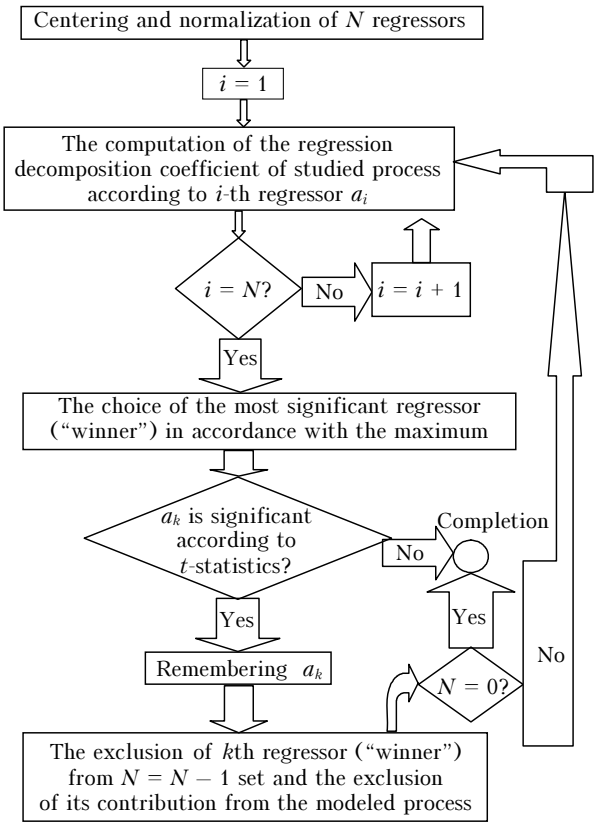

Fig. 3. The process chart of the regressive model building for the case when the number of regressors exceeds the number of readings.

The process of building the model was implemented in two variants:

– regressors' values referred to the same month as values of modeled process (synchronous model);

– regressors' values were taken for the preceding month (a month lag).

3. Modeling results

The results of aerosol scattering coefficient modeling are illustrated in Fig. 4.

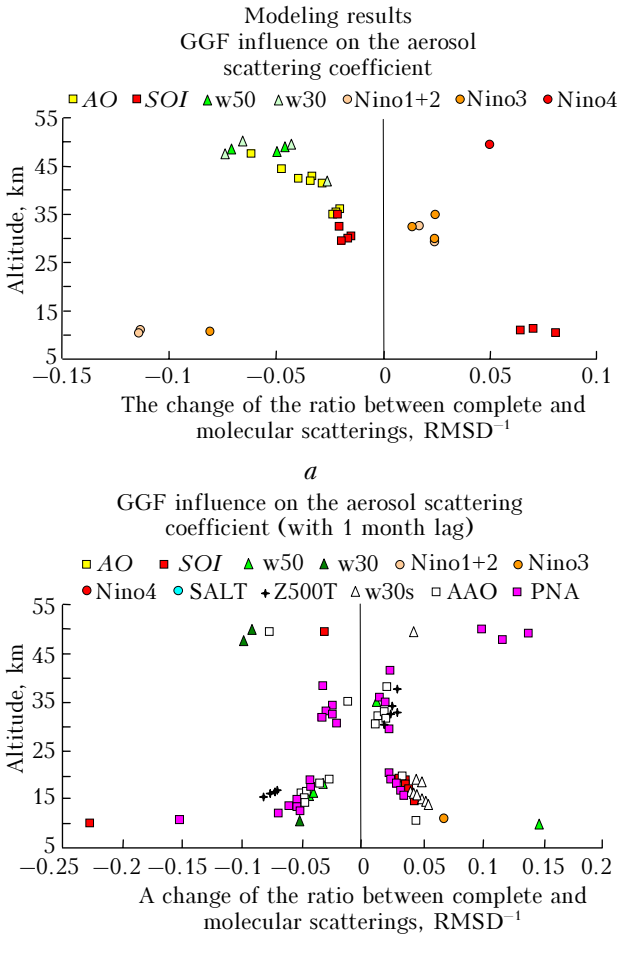

Fig. 4. Modeling results of GGF influence on aerosol scattering profiles: synchronous model (*a*); a model with 1 month lag (*b*).

To compare the influence of different GGFs, changes in the ratios between complete and molecular scatterings were normalized to the root-mean-square deviation (RMSD). It is seen in Fig. 4 that most GGFs influence the state of aerosol layer over West Siberia with a certain lag. Moreover, from a physical point of view this effect is natural, because the centers of action of most GGFs are situated in the equatorial zone. As for the synchronous model (the first variant) its regressive relations are governed not by the cause-and-effect relation mechanism (GGF changes influence the aerosol), but by the fact that synchronous changes in GGF and the state of aerosol layer over West Siberia are the effects of one and the same cause. The cause-and-effect relations are intrinsic to the second model (with the lag). The correlation between observable and model profiles is illustrated in Fig. 5.

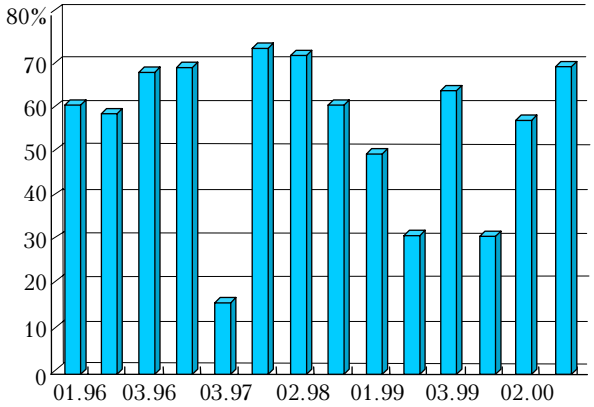

Fig. 5. The correlation of the model with month-averaged profiles of AVR.

It is seen that on the whole the correlation is sufficient, excluding some months (March, 1997; February, 1999; January, 2000). To elucidate the cause of this effect, a model of albedo seasonal behavior in the Tomsk Region was built (Fig. 6) according to the TOMS (Total Ozone Measurement System reflectivity) measurements; and the deviations from this model have been analyzed (Fig. 7) (TOMS is a satellite equipment for measuring the total ozone content, reflectivity, and aerosol index. This device is in use (with short breaks) at different Space systems since the end of October, 1978).

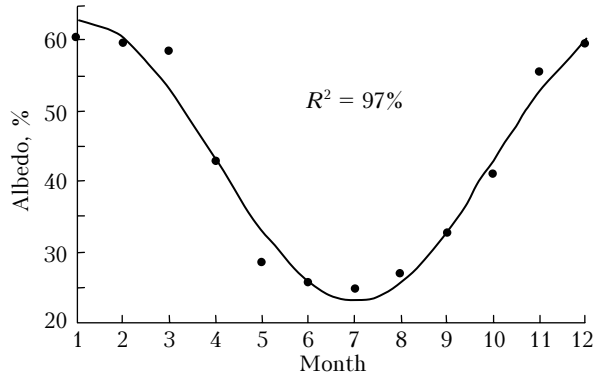

Fig. 6. Albedo behavior in the Tomsk Region: the curve is first harmonic of a seasonal behavior; • – month-average values.

Figure 6 shows the magnitude of the determination coefficient defined as $R^2 = 1 - \sigma^2_{\text{rest}}/\sigma^2_u$ (where σ^2_u and σ^2_{rest} are the series and model remnant dispersions), which characterizes the model quality.

The analysis evidences that positive albedo anomalies, which accompany cyclonic circulation in Tomsk Region, correspond to low correlation values for the model and observable aerosol scattering profiles. This fact allows the following conclusions about the influence of GGF on AVR:

– GGF has a significant influence on formation of AVR profiles over West Siberia and determines about one third of their variability;

– the altitude range of GGF influence consists of two regions: 28 km region and a region lower than 23 km, in which GGF is mainly in anti-phase;

– in conditions of the cyclonic circulation the influence of GGF decreases significantly.

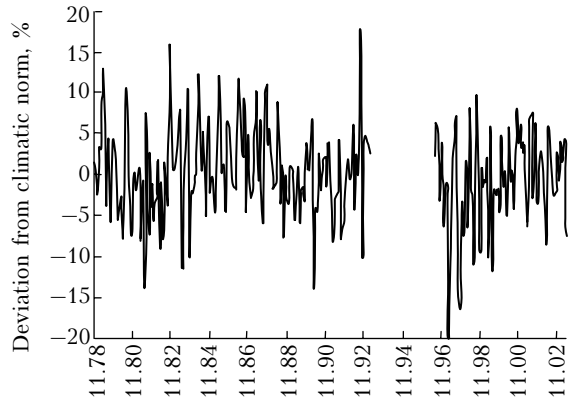

Fig. 7. The deviation of Tomsk Region albedo from a climatic norm.

The modeling of GGF influence on OVD and TVD by the first variant was made earlier.[1] The quality of modeling by the second variant is presented in Figs. 8 and 9.

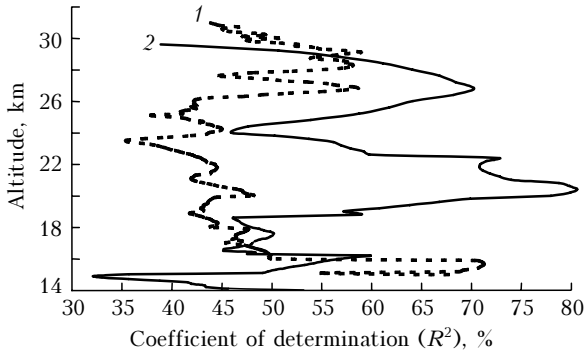

Fig. 8. Comparative efficiency of OVD and TVD regressive modeling: temperature (*1*); ozone (*2*).

The total efficiency of regression model for ozone and temperature has a mean value of 50% by altitude. Figure 10 shows the influence of an altitude behavior of model regression coefficients of OVD and TVD on the values of GGF with month lag (i.e., connected by the cause-and-effect relation with ozone and temperature variations).

It is seen that the stratosphere temperature variation over West Siberia in a wide range of stratospheric altitudes is formed due to variations in zonal component of equatorial wind at a level of 50 mbar. This is not surprising, because it is known that the stratospheric warming and cooling are directly related to quasi-two-year variations of this component. Note a significant magnitude of the regression coefficient from 5 to 6.5 °C on RDMS. It means that QBO is responsible for a greater dynamic range of the temperature variation in the lower stratosphere over West Siberia.

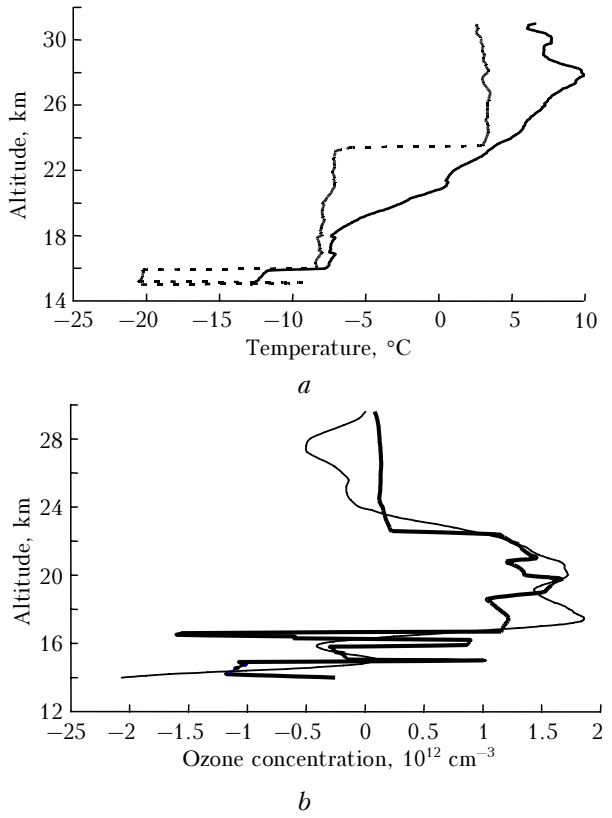

Fig. 9. A comparison of a model with TVD: remnants of seasonal behavior (solid line), model (dot line) and OVD (*a*); remnants of seasonal trend (thin line) and a model (bold) in 1996 (*b*).

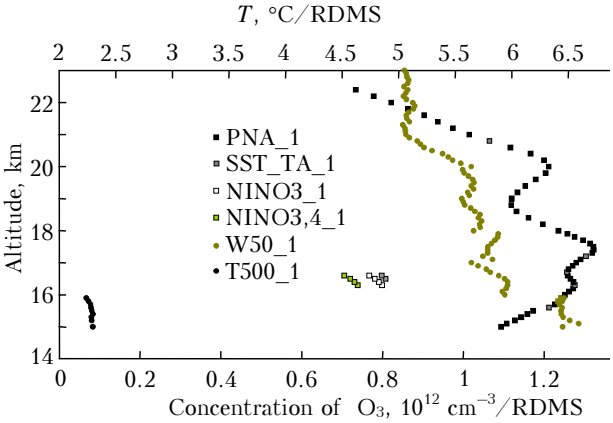

Fig. 10. The modeling results of GGF values influence on OVD and TVD with 1 month lag. Grey signs indicate the temperature response and black squares indicate the ozone response.

A small altitude range near tropopause undergoes the influence of mean global temperature at a level of 500 mbar, that is also natural.

The index of North Pacific variation is the main factor, which determines ozone variation in a wide altitude range. This fact also has a reasonable explanation: the index substantially determines the position of circumpolar vortex. The fact that a small altitude range between 16 and 17 km undergoes the

influence of World Ocean surface temperature at such water areas, as tropical Atlantic and western part of sub-equatorial zone of the Pacific, deserves a special discussion. Generally, the fact that the temperature increase leads to an increase in ozone concentration in the lower part of OVD climatic maximum (Fig. 11) allows us to make a supposition that tropospheric upward air currents over the above mentioned water areas are closed over West Siberia. In this case a downward current leads to an increase in ozone concentration according to Norman–Dobson principle. Such mechanisms, as applied to these water areas, are discussed in Ref. 2, which is dedicated to the analysis of El-Nino influence on processes in ozonosphere.

However, a small altitude range, in which the temperature influence of tropical water areas of the World Ocean manifests itself, as well as an insignificant amount of experimental data for the creation of regressive model do not allow us to substantiate such a conclusion.

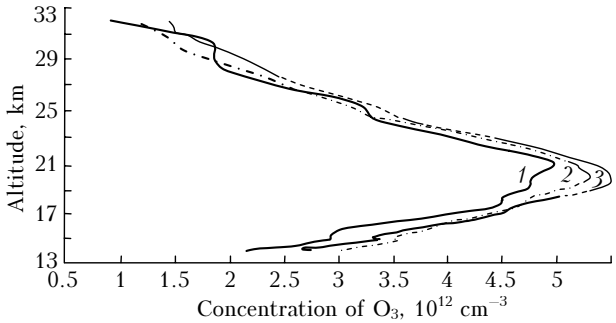

Fig. 11. Averaged OVD in the lower troposphere over Tomsk: January (*1*); February (*2*); March (*3*) [Ref. 1].

References

1. V.N. Marichev, I.L. Galkina, and G.M. Kruchenitskii, Meteorol. i Gidrol., No. 11, 44–53 (2003).
2. A.A. Chernikov, Yu.A. Borisov, A.M. Zvyagintsev, G.M. Kruchenitskii, S.P. Perov, N.S. Sidorenkov, and O.V. Stasyuk, Meteorol. i Gidrol., No. 3, 104–110 (1998).